

## Efficient CO<sub>2</sub> absorption in aqueous dual functionalized cyclic ionic liquids

Surya Chandra Tiwari, Kamal Kishore Pant \*, Sreedevi Upadhyayula \*

Department of Chemical Engineering, Indian Institute of Technology Delhi, Hauz Khas, New Delhi, 110016, India

### ARTICLE INFO

**Keywords:**

Functionalized ionic liquids  
CO<sub>2</sub> capture  
NMR characterization  
Absorption kinetics and mechanism  
Cyclic regeneration

### ABSTRACT

Novel dual functionalized ionic liquids were synthesized using four different cyclic anions, azolide/ piperazine, in combination with triethylenetetramine cation. These ionic liquids were used to absorb CO<sub>2</sub> in aqueous form at 300 K and ambient pressure and [TETAH][Pz], [TETAH][Im], [TETAH][Py] and [TETAH][Tz], showed 2.05, 1.81, 1.73 and 1.50, CO<sub>2</sub> loading in mol of CO<sub>2</sub> / mol ionic liquids, respectively, higher than industrial amine absorbents like monoethanolamine, which have 0.65–0.68 mol of CO<sub>2</sub> / mol. Based on kinetics of CO<sub>2</sub> absorption, Hatta number was calculated for comparative a study, and it showed that high interfacial area is favorable for higher absorption rate. Aqueous [TETAH][Im] and [TETAH][Py] showed high basicity and good yields of carbamate in these two DFILs. <sup>13</sup>C NMR results suggest that steric hindrance effect decreased in aqueous medium, and the reaction of piperazine anion with CO<sub>2</sub> and [TETAH][Pz] resulted in higher CO<sub>2</sub> loading. Bond length and angle of CO<sub>2</sub> -amines system was calculated by geometry optimization simulation and shows attraction of CO<sub>2</sub> is higher in [Pz] anion. Regeneration cyclic efficiency was found to be around 90–95 % for multiple absorption desorption cycles with negligible absorbent loss.

### 1. Introduction

Flue gas effluent streams from industries contain greenhouse gas CO<sub>2</sub> which is the major source of air pollution in urban areas [1]. The major sources of CO<sub>2</sub> emission are uncontrolled combustion of fossil fuels such as coal, natural gases, and petrochemicals [2]. Researchers are attempting to develop suitable technologies to capture and store/ utilize this carbon dioxide. There are several technologies for CO<sub>2</sub> capture and utilization of which absorption into suitable solvents is the most common industrial process due to bulk CO<sub>2</sub> capturing capacity [3]. Alkanolamines based aqueous solutions are used by most of the industries for CO<sub>2</sub> absorption. However, alkanolamines based absorption has several drawbacks, such as, high vapor pressure of the solvent system, corrosive nature, and high regeneration cost [4,5]. These problems can be overcome by developing cost-effective, energy-efficient, and less corrosive solvent systems.

Ionic liquids (ILs) have a great potential to replace these alkanolamines for CO<sub>2</sub> capture, due to their exciting properties like low vapor pressure, low corrosion of equipment, high thermal stability, and conductivity [6,7]. ILs can be developed for any particular application based on specific property and structure-activity relationships [8]. Initially, various ILs have been reported as physical solvents for CO<sub>2</sub> absorption, however, the highest CO<sub>2</sub> capture reported in these physical

solvents is around (0.5–1.0) mol/ mol IL [9,10]. Later, functionalized ionic liquids (FILs) were developed as chemical absorbents for CO<sub>2</sub> with active functional groups (especially, amine and amino groups) to form carbamates [11,12]. These functionalized ionic liquids are synthesized using combinations of amine/ amino group-based anion and cation. FILs containing amino groups are typically synthesized using amino acid anion [13,14]. A series of 20 dual-amino functionalized phosphonium ILs were synthesized and studied by Y. Zhang et al. [15]. The CO<sub>2</sub> was found to be chemically absorbed in [aP<sub>4443</sub>][Gly] and [aP<sub>4443</sub>][Ala] upto a loading of 1 mole CO<sub>2</sub>/ mole IL approximately. In 2016, B. Lv et al. and Z. Zhou et al. synthesized imidazolium, and amino acid based [Apmim][Lys] and [Apmin][Gly] dual-functionalized ionic liquids (DFILs) and found that their CO<sub>2</sub> loading capacity to be almost 1.80 and 1.23 mole CO<sub>2</sub>/ mole IL, at 303 K and ambient pressure [16,17]. J. Albo et al. used [EMIM][EtSO<sub>4</sub>] ionic liquid for CO<sub>2</sub> capture with cross flow membrane contactor, in which CO<sub>2</sub> recovery was reported to be in the range of 8–41 % and the value of mass transfer coefficient is determined to be  $3.78 \times 10^{-6}$  m.s<sup>-1</sup>, which is five times higher than macroscopic study [18,19]. Further, two [emim] cation based ILs were used for CO<sub>2</sub> capture and the results show that around 90 % membrane absorber efficiency can be obtained in the absorption/ desorption setup [20].

Although reports have shown that FILs using amino groups showed promise in CO<sub>2</sub> capture in comparison to industrial solvents, yet, there is

\* Corresponding authors.

E-mail addresses: [kkpant@chemical.iitd.ac.in](mailto:kkpant@chemical.iitd.ac.in) (K.K. Pant), [sreedevi@chemical.iitd.ac.in](mailto:sreedevi@chemical.iitd.ac.in) (S. Upadhyayula).

still an issue of low CO<sub>2</sub> solubility [21]. CO<sub>2</sub> solubility is increased with increasing amine functionality, however, the steric hindrance effect also increases with the number of groups added to the ILs [22]. Moreover, amino group based FILs form a strong hydrogen bond network with CO<sub>2</sub>, raising the viscosity and energy required for regeneration [23]. Researchers have reported that most of the ionic liquids have higher viscosities than alkanolamine solutions rendering them uneconomical for bulk CO<sub>2</sub> capture [24]. Recently, researchers identified that certain concentrations of ionic liquids in aqueous solution give excellent CO<sub>2</sub> absorption performance due to significant viscosity reduction in aqueous solution [25,26]. A series of dual site imidazolium-based phenolate ILs were used in an ionic liquid membrane and high selectivity of CO<sub>2</sub>/ N<sub>2</sub> of 135 and 127 for neat and aqueous solution, respectively, is reported [27]. The ionic liquid membrane based on [emim][ac] shows high activation energy for N<sub>2</sub> permeability, and with Al<sub>2</sub>O<sub>3</sub>/ TiO<sub>2</sub> support it can be operated at high temperature up to 150 °C [28,29].

A new class of ILs called protic/ aprotic ionic liquids (PILs) have attracted many researchers due to their relatively low cost and ease of synthesis, and tunable properties towards CO<sub>2</sub> absorption [30,31]. Wang et al. synthesized aprotic ionic liquids (AILs) using azolide anion and phosphonium cation, and investigated their CO<sub>2</sub> absorption capacity, and found that they have low enthalpy of absorption and showed recyclability up to 25 times with minor losses [32]. X. Zhang et al. synthesized azole-derived PILs and the results show that absorption selectivity H<sub>2</sub>/ CH<sub>4</sub> and CO<sub>2</sub>/ CH<sub>4</sub> is high in these PILs [33]. Diamino protic ionic liquids (DPILs) were synthesized by Simons et al. using formate anion which showed low volatility than aminoethanol amines and also good CO<sub>2</sub> loading (almost 12 w/w %) [34]. In 2018, T. Oncsik et al. synthesized a series of lower molecular weight DPILs based on azolide anions such as [DMAPAH][Im] and [DMEDAH][Py]. Their results revealed high CO<sub>2</sub> loading (22.2 w/w %) and almost complete solvent regeneration at low temperature (323 K) under N<sub>2</sub> atmosphere. This is due to the presence of an azolide anion, which has weak hydrogen bonding with nitrogen [35]. In 2019, J. Wu et al. synthesized a series of DFILs, in which polyamine diethylenetriamine (DETA) was used as a cation and azolide as an anion. Their DFT calculations (reaction enthalpy -20 KJ) showed that the formation of DFILs could be possible by acid-base neutralization reaction. This result indicates that specific polyamines could be protonated by less stable azolide to form DFILs [36].

An efficient strategy to improve the CO<sub>2</sub> solubility in FILs is increasing the number of amine groups, however, formation of stable carbamates restricts solvent regeneration. Azolide based FILs form fewer stable carbamates, which is favorable for solvent regeneration. Y. Sun. et al. synthesized DFILs with triethyltetramine TETA cation and azolide (imidazole and pyrazole) anion and used them for NO absorption successfully [37]. In this work, TETA polyamine has been used as a cation with an azolide or piperazine anion to form DFILs. TETA bears three ethylene and four amine groups (primary and secondary amine groups) in which the long chain of ethylene and amines favor high CO<sub>2</sub> loading [38]. Piperazine is a cyclic amine used as a promoter for CO<sub>2</sub> capture due to its reactive nature and can be easily deprotonated when reacting with CO<sub>2</sub> in an aqueous medium. These results encourage the use of piperazine as an anion to form DFILs [39,40].

Herein, DFILs were synthesized based on TETA cation and cyclic amine (imidazole, pyrazole, triazole, and piperazine) anions, and CO<sub>2</sub> absorption in these aqueous solvents is investigated. The DFILs were characterized using NMR, FTIR, TGA and their properties, such as thermal stability and viscosity were analyzed. CO<sub>2</sub> absorption and kinetics were investigated in a laboratory set-up shown in SI-1 and the influence of physicochemical properties and alkalinity on the CO<sub>2</sub> absorption into the aqueous DFILs is studied. Further, a mechanism of CO<sub>2</sub> absorption was proposed based on the analysis results from <sup>13</sup>C NMR. A geometry optimization simulation technique was used to study the affinity of CO<sub>2</sub> toward these anions. The regeneration performance of the

aqueous DFILs was assessed after conducting absorption experiments in multiple regeneration cycles.

## 2. Materials and methods

### 2.1. Materials

Triethylenetetramine (TETA, ≥ 97.0 %), piperazine (Pz, ≥ 98.0 %), 1,2,4-triazole (Tz, ≥ 99.0 %), pyrazole (Py, ≥ 98.0 %), Imidazole (Im, ≥ 98.0 %), ethanol (EtOH, ≥ 99.90 %), CO<sub>2</sub> gas cylinder (CO<sub>2</sub> ≥ 99.80 %) were purchased from Sigma Aldrich, India. Deuterium oxide (D<sub>2</sub>O ≥ 99.99 %), was purchased from Central Drug House Pvt. Ltd., India. All chemicals were used without further purification. The structures of cations and anions used in the synthesis of DFILs are shown in Fig. 1.

### 2.2. Synthesis and characterization of dual functionalized ionic liquids (DFILs)

The DFILs [TETAH][Pz], [TETAH][Tz], [TETAH][Py] and [TETAH][Im] were directly synthesized by acid-base neutralization reaction following the procedure mentioned in literature for DFILs by Y. Sin et al. [37]. Considering [TETAH][Pz], for instance, an equimolar amount of [TETA] and [Pz] were mixed (stirring 500 rpm) in a round bottom flask at 300 K with a sufficient amount of the ethanol-water solvent (4:1, V/V) for 24 h. This is gently concentrated in a vacuum rotary evaporator at 333 K temperature and 55 mbar pressure. The spectroscopic analyzer <sup>1</sup>H NMR and ATR-FTIR was employed to analyze the chemical structure of DFILs, which were provided and discussed in the Supporting Information (SI). T. Oncsik et al. [35] and J. Wu et al. [36] reported <sup>1</sup>H and <sup>13</sup>C NMR of DFILs analyzed on a Bruker Advance (400 MHz) using D<sub>2</sub>O as the reference solvent. The ATR-FTIR sampler in Thermo-Nicolet (iS05) was used to record the infrared spectra in the range of 450–4000 cm<sup>-1</sup>. Additionally, thermal stability of DFILs was studied in the temperature range of 300–520 K under N<sub>2</sub> (30 mL/ min) at a heating rate of 10 K / min using TGA instrument Model-S.D.T., Q 600. The TGA data of DFILs is shown in the Supporting information.

### 2.3. Measurement and calculation of physicochemical properties

#### 2.3.1. Viscosity

The viscosity of as-synthesized and aqueous DFILs was measured using a Rheometric viscometer Model M-302, Anton Paar varying the temperature. The viscosity-temperature characteristics of the DFILs can be explained by an extended Arrhenius law [41] given by the following equation:

$$\ln \mu = \frac{E_a}{RT} + \ln \mu_0 \quad (1)$$

E<sub>a</sub> is activation energy and directly correlates to the heat of vaporization of DFILs, μ<sub>0</sub> is empirical constant and can be correlated to vapor phase viscosity of the DFILs, and R is gas constant.

Based on E<sub>a</sub> and molar volume (V<sub>IL</sub>), S.S. Moganty et al. [42], was proposed a mathematical correlation to calculate Hildebrand solubility parameter (δ<sub>IL</sub>), which correlation is given by following equation:

$$\delta_{IL} = \sqrt{\frac{4E_a}{V_{IL}}} \quad (2)$$

#### 2.3.2. Diffusion coefficient

The aqueous DFILs act as an electrolyte solution. Therefore, CO<sub>2</sub> diffusivity in aqueous DFILs can be calculated based on X. Zhou et al. [43] work and the following equation:

$$D_{CO_{2,IL}} = D_{CO_{2,w}}(1 - KC) \quad (3)$$

$$D_{CO_{2,w}} = 2.35 * 10^{-6} \exp\left(\frac{-2119}{T}\right) \quad (4)$$

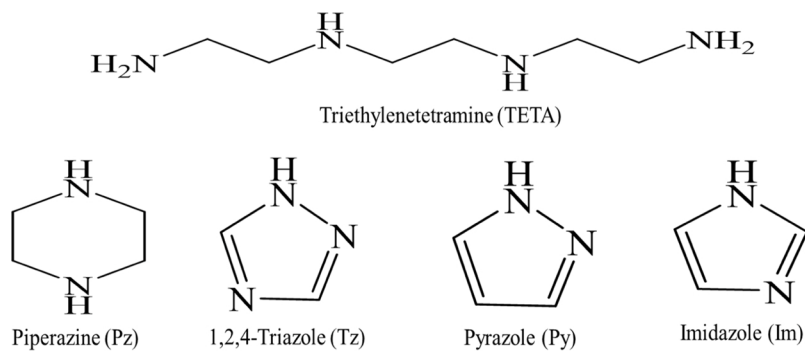


**Fig. 1.** Structure of the cations and anions used for DFILs synthesis.

$D_{CO_2,w}$  and  $D_{CO_2,IL}$  are the CO<sub>2</sub> diffusion coefficient in water and aqueous DFILs, respectively, C is the concentration of DFILs and K is constant, which can be calculated by following expression:

$$K = 0.03 + 0.55\omega \quad (5)$$

Where,  $\omega$  depends on the viscosity of water ( $\mu_w$ ) and aqueous DFILs solution ( $\mu_{IL}$ ) respectively and can be obtained by the following equation:

$$\mu_w = \mu_{IL}(1 - \omega C) \quad (6)$$

Thus, CO<sub>2</sub> mass diffusion coefficient (CO<sub>2</sub> diffusivity) in aqueous DFILs solution can be calculated by the following simplified equation:

$$D_{CO_2,IL} [2.35 * 10^{-6} \exp \left( \frac{-2119}{T} [0.45 - 0.03C + .55 \left( \frac{\mu_w}{\mu_{IL}} \right)] \right) \quad (7)$$

### 2.3.3. Dissociation constant measurement

The pH value of aqueous DFILs was measured by a pH meter CyberScan 510 of Thermo Fisher Scientific Inc. (India). The uncertainty of pH meter was  $\pm 0.05$  and  $\pm 0.02$  for the pH range of 10–13 and 4–9 respectively. The dissociation constant (pKa) was determined typically from Eq. (17) as also reported by S. Liu et al. [44,45]. When aqueous solutions of the DFILs are prepared, the following equilibrium reactions take place: the decomposition of water, protonation of DFIL, and hydrolysis of DFIL, as shown in Eqs. (8)–(10), respectively.



DFIL and DFILH<sup>+</sup> are respectively dual functionalized ionic liquid and protonated IL in the presence of water,  $K_w$ ,  $K_a$ ,  $K_e$  are equilibrium constants in each of the three reactions, respectively. Applying mole and charge balance on the Eqs. (8)–(10):

$$[DFIL]_o = [DFIL] + [DFILH^+] \quad (11)$$

$$[DFILH^+] + [H^+] = [OH^-] \quad (12)$$

$$K_w = [H^+] [OH^-] \quad (13)$$

$$K_a = \frac{[DFIL][H^+]}{[DFILH^+]} \quad (14)$$

Here, initial molar concentration is represented as [DFIL]<sub>o</sub> and the free molar concentration of as-synthesized DFILs present in the solution is represented as [DFIL]. The amount of [H<sup>+</sup>] is very less compared to [OH<sup>-</sup>] in aqueous DFILs and hence, molar concentrations of [OH<sup>-</sup>] should be approximately equal to molar concentration of [DFILH<sup>+</sup>].

$$[DFILH^+] \approx [OH^-] \quad (15)$$

Therefore, Eq. (14) could be rearranged by substituting [DFIL], and [DFILH<sup>+</sup>] value from the Eqs. (11),(15) and (13) respectively. Hence, ionization constant ( $K_a$ ) and dissociation constant (pKa) can thus be calculated as:

$$K_a = \left\{ \left( \frac{[DFIL]_o [H^+]}{K_w} - 1 \right) * [H^+] \right\} \quad (16)$$

$$pKa = -\log K_a \quad (17)$$

where,  $K_w$ , [DFIL]<sub>o</sub> and [H<sup>+</sup>] can be determined by temperature setting ( $K_w$  is  $1.20 * 10^{-14}$  at given condition), initial solution concentration, and known pH value, respectively.

### 2.4. CO<sub>2</sub> absorption and desorption measurements

The experimental setup for CO<sub>2</sub> absorption and desorption measurements consists of a round bottom flask with a reflux condenser. The measurement was performed by passing a high-grade CO<sub>2</sub> gas stream with a flow rate of 30 mL/min into a round bottom bubbler reactor of 25 ml capacity containing 0.5 mol /l DFILs aqueous solution (absorbent) at room temperature (300 K) and ambient pressure (1 atm). The experimental setup is shown in Fig. SI-1. The weight change was detected by an electronic analytical balance having an accuracy of  $\pm 0.1$  mg until equilibrium solubility was achieved. The weight increment was attributed to the absorbed CO<sub>2</sub>, and the amount of absorbed CO<sub>2</sub> was calculated directly following the method used by M. Xiao et al. [46]. To check the reproducibility, the experiments were repeated 3 times with confidence limits  $\pm 3\%$ . The CO<sub>2</sub> absorption kinetics were investigated and the rate equation for absorption is as follows:

$$-r_a = \frac{-1}{V_r} \frac{dn}{dt} \quad (18)$$

$$-\log \frac{[n_t - n_e]}{[n_0 - n_e]} = K_{app} t \quad (19)$$

$V_r$ ,  $n_t$ ,  $n_e$ , and  $n_0$  is volume of absorbent, mole of CO<sub>2</sub> absorbed at any time t, equilibrium, and initial, respectively.

All the experiments for CO<sub>2</sub> desorption and regeneration of the aqueous DFILs were performed at 393 K with a stirring speed of 450 rpm. A reflux condenser was used at the mouth of the round bottom flask to avoid the loss of absorbents.

### 2.5. Geometry optimization

The bond length, bond gap, and bond angle of selected molecules were calculated based on energy minimization, followed by geometry optimization. Material Studio (M.S.) software 2017, provided by BIOVIA, was used for this simulation. The calculation was performed by

using the DMOL3 module and B3LYP/6-311++G\*\* basis [47].

### 3. Results and discussion

#### 3.1. Physical properties and stability of DFILs

Viscosity is a crucial physical property of liquid, especially for ionic liquids. Lower viscosity is always favorable for CO<sub>2</sub> absorption because the resistance to mass transfer increases with high viscosity. Ionic liquids are reported to more viscous than conventional solvents such as amines, with their viscosities lying in the range of 7–1800 mPa·s [48]. Viscosity of DFILs was measured over the temperature range of 300 K–350 K, and is included in Table SI-2, wherein, it is seen that the viscosity is lower compared to magnetic ionic liquids and protic ionic liquids [49,50]. As evident from the table, viscosity of as-synthesized DFILs is decreasing significantly with increasing temperature due to increased movement of molecules resulting in bond weakening/ breaking between cation and anion. The viscosity of as-synthesized DFILs was found to be in the order: [TETAH][Tz] > [TETAH][Pz] > [TETAH][Py] > [TETAH][Im], as shown in Fig. 2. The thermal stability of DFILs is also found in a similar order and is shown in Fig. SI-5. The extensive hydrogen bonding network between N-H—N molecules and a higher number of nitrogen atoms may be responsible for higher viscosity of [TETAH][Tz]. This result reveals that anion has a crucial role in the enhancement of viscosity. The viscosity-temperature characteristics of the DFILs can be explained by an extended Arrhenius law given by Eq. (1).

A plot of ln μ vs 1/T presents a good linear relationship, as shown in Fig. 3. From the graph, the values of E<sub>a</sub>, μ<sub>0</sub>, and R<sup>2</sup> are listed in Table 1. Based on E<sub>a</sub> results, it can be predicted that the heat of vaporization of DFILs can be following a sequence: [TETAH][Pz] > [TETAH][Tz] > [TETAH][Im] > [TETAH][Py]. Therefore, the hydrogen bonding strength should be high in [TETAH][Pz]. Based on TGA results (shown in Fig. SI-5), the temperature at which 50 % mass loss (designated as thermal decomposition temperature) of DFILs is shown in Table 1. The TGA results are shown in Fig. SI-5 and suggest that the DFILs have good enough stability for the CO<sub>2</sub> absorption process. There is no significant weight loss of these DFILs until 390 K, hence, the regeneration temperature of these DFILs can be done in 348–390 K temp range, the thermal decomposition temperature is highest for [TETAH][Tz] and δ<sub>IL</sub> is a crucial parameter to investigate cohesive energy density [31,51] for DFILs, and it can be calculated from Eq. (2) by using E<sub>a</sub> at 300 K, are shown in Table 1. The cohesive energy density sequence of DFILs is as follow: [TETAH][Pz] < [TETAH][Py] < [TETAH][Tz] < [TETAH][Im]. The results confirm that the δ<sub>IL</sub> is inversely proportional to molecular weight of compound. Therefore, based on δ<sub>IL</sub> value intermolecular

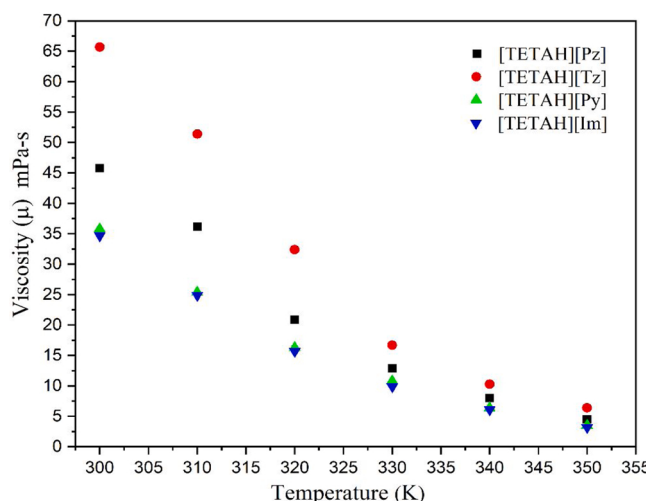


Fig. 2. Viscosity of the DFILs in the temperature range of 300–350 K.

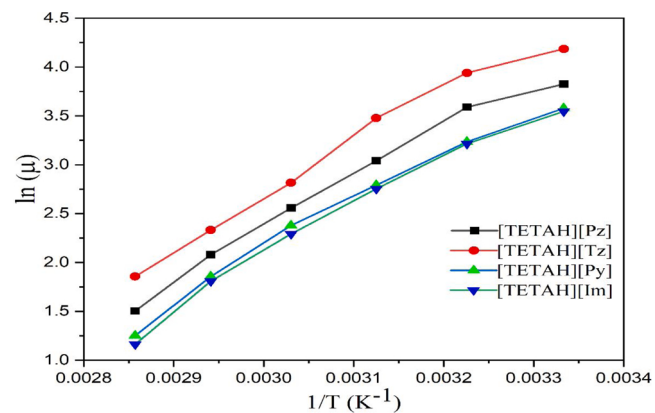


Fig. 3. Arrhenius plot for viscosity change with temperature for the DFILs.

Table 1

Arrhenius constants for viscosity variation with temperature for the DFILs.

Absorbent	E <sub>a</sub> (kcal/ mol)	μ <sub>0</sub> * 10 <sup>-6</sup> (mPa· s)	(%) R <sup>2</sup>	V <sub>IL</sub> (cm <sup>3</sup> / mol)	δ <sub>IL</sub> (J/ cm <sup>3</sup> ) <sup>1/2</sup>	Temperature (K) <sup>#</sup>
[TETAH] [Pz]	9.86	3.57	98.159	230.06	26.78	417.54
[TETAH] [Tz]	10.17	3.08	98.157	219.62	27.84	448.60
[TETAH] [Py]	9.59	4.20	98.160	211.17	27.57	414.55
[TETAH] [Im]	9.85	2.69	98.161	210.42	27.99	416.03

<sup>#</sup> Thermal decomposition temperature).

attractive force is high in [TETAH][Im] and low in [TETAH][Pz].

#### 3.2. CO<sub>2</sub> absorption in aqueous DFILs and its kinetics

The CO<sub>2</sub> was absorbed in aqueous DFILs at room temperature (300 K) and 1 atm pressure under a constant stirring rate of 430 rpm. The CO<sub>2</sub> loading was analyzed after every 10 min time intervals, and it is shown in Fig. 4. Due to the zwitterion mechanism, DFILs have an ability to absorb an equimolar amount of CO<sub>2</sub> in an aqueous medium [34]. The CO<sub>2</sub> loading is 2.05, 1.50, 1.73 and 1.81 mol CO<sub>2</sub>/ mol IL, for [TETAH][Pz], [TETAH][Tz], [TETAH][Py] and [TETAH][Im] DFILs respectively. This high CO<sub>2</sub> loading in these DFILs is attributed to the formation of

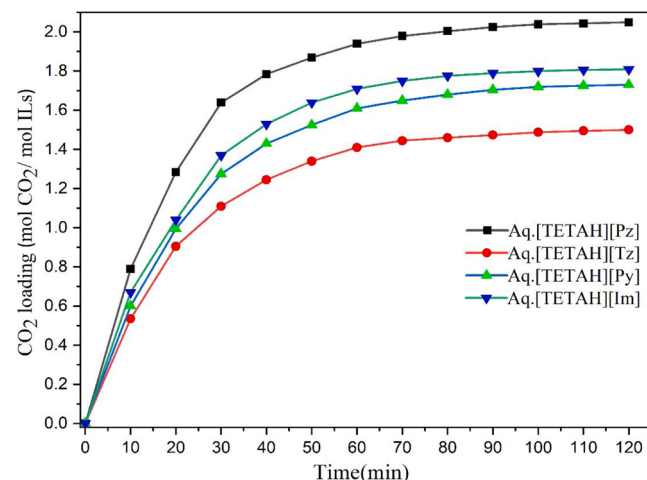


Fig. 4. CO<sub>2</sub> absorption in aqueous DFILs (300 K and ambient pressure).

carbamates as well as bicarbonate by the reaction of cation and CO<sub>2</sub>, and anion, water, and CO<sub>2</sub>, respectively. This result indicates that to enhance CO<sub>2</sub> loading rate in DFILs, role of anion is important, and here, the anions showed the following order in CO<sub>2</sub> loading [Pz] > [Im] > [Py] > [Tz]. [Pz] anion based DFILs showed highest CO<sub>2</sub> loading due to the highly reactive nature of piperazine which readily forms carbamates in an aqueous medium compared to azoles. A comparison of CO<sub>2</sub> absorption in these aqueous DFILs with literature is shown in Table 2. It can be seen from the table that the CO<sub>2</sub> loading in [TETAH][Pz] at 300 K is better than that reported for [DETAH][Tz], [DETAH][Gly] at 313 K.

The table also shows that [TETAH][Im], [TETAH][Py] has better CO<sub>2</sub> absorption on mass as well as mole basis. Comparing with the work of P. W. J. Derk et al., [52] and S.K. Dash et al. [53] who have reported CO<sub>2</sub> solubility in aqueous piperazine at different temperature and pressure, it can be seen from Table 2 that CO<sub>2</sub> solubility in a 0.5 mol/l aqueous DFILs solution is higher than that in a 0.6 mol/l of aqueous piperazine on mole basis.

The CO<sub>2</sub> absorption kinetics follow Eqs. (18)–(19) and the CO<sub>2</sub> absorption was found to decrease with increasing time due to reduced active site density in the DFILs. An apparent rate constant ( $K_{app}$ ) was determined from a logarithmic plot of CO<sub>2</sub> loading with time, as shown in Fig. 5. The rate constant show the following order: [TETAH][Pz] > [TETAH][Im] > {TETAH}[Py] > [TETAH][Tz].

The initial rate of CO<sub>2</sub> absorption is higher in aq. [TETAH][Pz], which is attributed to the rapid reactive nature of Pz anion with CO<sub>2</sub> in aqueous medium. The CO<sub>2</sub> absorption rate is low in aq. [TETAH][Tz] as the mass transfer resistant is high and also due to the low reactivity of Tz anion.

The effect of temperature on CO<sub>2</sub> loading in aqueous DFILs is investigated at 300 and 310 K and atmospheric pressure, and is shown in Fig. 6. The results reveal that CO<sub>2</sub> loading decreases from 2.05 to 1.96 mol CO<sub>2</sub> / mol ILs for aq. [TETAH][Pz] with increase in temperature from 300 to 310 K, respectively. As absorption is an exothermic process and the formation of carbamates decreases with increasing temeprature, a reduction of CO<sub>2</sub> loading is observed when temperature is increased as also reported by M. Xiao et al. in their research work [46].

### 3.3. Alkalinity of aqueous DFILs and CO<sub>2</sub> diffusivity

Acid dissociation constant (pKa) is a key factor to identify the alkalinity of a solution, and it is also a fundamental property of aqueous solvent affecting the CO<sub>2</sub> absorption and kinetics [54–56]. The role of pKa value is crucial to the selection of solvent for CO<sub>2</sub> absorption [44, 45]. The pKa values of aqueous DFILs were calculated from Eq. (17) and are given in Table 3. The pH values of aqueous DFILs and de-ionized water, before and after CO<sub>2</sub> loading, were measured at 300 K and ambient pressure and shown in Fig. 7. The alkalinity of aqueous DFILs follows the order: [TETAH][Im] > [TETAH][Py] > [TETAH][Pz] >

**Table 2**  
CO<sub>2</sub> absorption loading in various DFILs and other solvents at atmospheric pressure.

FILs	M <sub>w</sub>	T(K)	n <sub>CO<sub>2</sub></sub> / n <sub>FILs</sub>	%w/w	Concentration
[TETAH][Pz] <sup>34</sup>	232.38	300	2.05	38.63	0.5 mol/l
[TETAH][Tz] <sup>34</sup>	215.31	300	1.50	30.65	0.5 mol/l
[TETAH][Py] <sup>34</sup>	214.32	300	1.73	35.52	0.5 mol/l
[TETAH][Im] <sup>34</sup>	214.32	300	1.81	37.16	0.5 mol/l
[DETAH][Tz] <sup>36</sup>	172.23	313	1.74	44.50	0.5 mol/l
[DETAH][Gly] <sup>36</sup>	178.24	313	1.81	37.60	0.5 mol/l
[DMAPAH][Im] <sup>35</sup>	170.26	295	0.75	21.00	As-synthesized
[DMAPAH][Py] <sup>35</sup>	170.26	295	0.79	22.60	As-synthesized
[DMAPAH][Tz] <sup>35</sup>	171.25	295	0.70	18.30	As-synthesized
[Apmin][Lys] <sup>17</sup>	296.63	303	1.80	26.70	0.5 mol/l
[Apmin][Gly] <sup>21</sup>	284.84	303	1.23	19.00	0.5 mol/l
Piperazine <sup>52</sup>	86.14	298	1.06	–	0.6 mol/l

<sup>#</sup> This work.

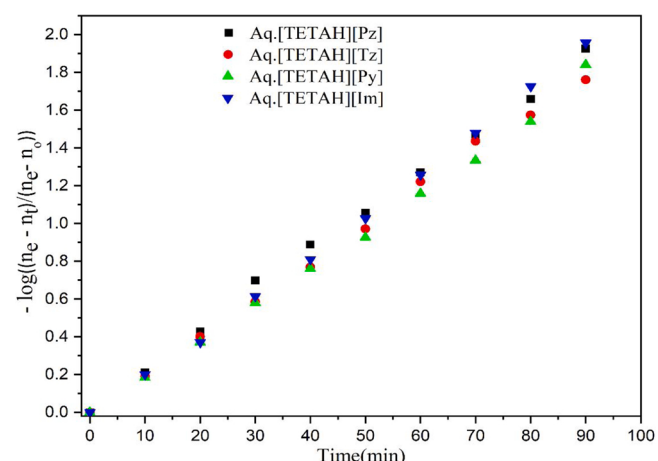


Fig. 5. CO<sub>2</sub> absorption rate plot for apparent rate constant ( $K_{app}$ ).

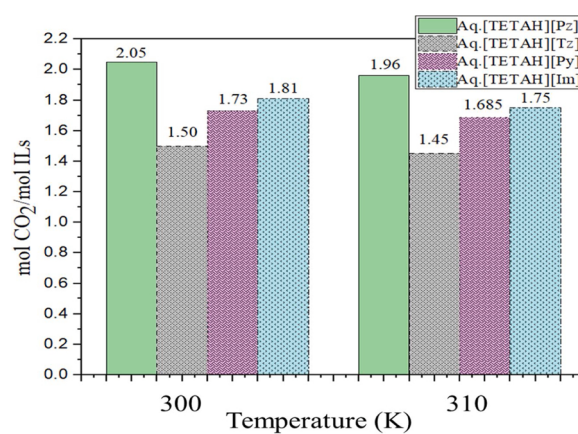


Fig. 6. Effect of Temperature on CO<sub>2</sub> loading in aqueous DFILs.

[TETAH][Tz]. This result indicates that the role of anion is crucial in increasing the alkalinity of the solution. Imidazole and pyrazole anion based DFILs gave higher pKa values 10.90 and 10.82, respectively. Additionally, the molar concentration of hydroxyl ion in aqueous DFILs was calculated before and after CO<sub>2</sub> loading by using Eq. (13), and is listed in Table 3. The interaction of hydroxyl ions with absorbent follows a similar trend as alkalinity. This result shows that the formation of bicarbonate is higher in [TETAH][Im] and [TETAH][Py] than in the other two aqueous DFILs and confirms that the formation of bicarbonates is low in triazole based DFILs leading to low CO<sub>2</sub> loading.

Viscosity of aqueous DFILs was measured over a temperature range of 300–320 K, and it followed a similar trend shown by as-synthesized DFILs as given in Fig. SI-6. Viscosity of DFILs in aqueous phase is significantly less than as-synthesized DFILs and almost equivalent to water. The CO<sub>2</sub> diffusivities are calculated from Eq. (7) using viscosity of absorbents at 300 K, and listed in Table 3. The CO<sub>2</sub> diffusivity follows the order: [TETAH][Im] > [TETAH][Py] > [TETAH][Pz] > [TETAH][Tz]. The CO<sub>2</sub> diffusivity is seen to be inversely proportional to viscosity as also reported by X. Zhou et al. [43]. The influence of CO<sub>2</sub> alkalinity and diffusivity on the absorption capacities is discussed in detail.

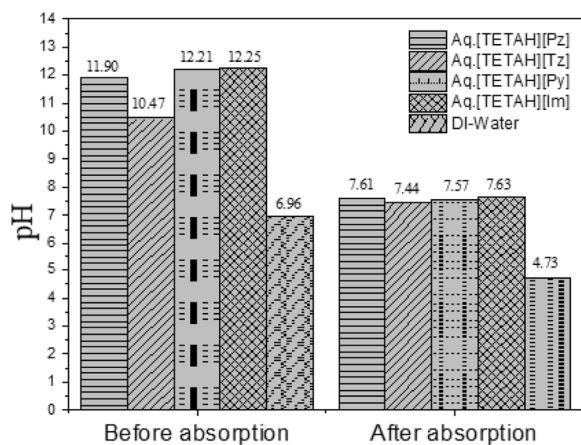
### 3.4. The influence of CO<sub>2</sub> alkalinity and diffusivity in the lab synthesized absorbents

The CO<sub>2</sub> absorption was performed in a bubble-type contactor. The resistance should be in bulk liquid in which mass transfer resistance and reaction rate resistance have a crucial role [57,58]. Therefore, to understand the mass transfer resistance in CO<sub>2</sub>- DFILs system, a plot

**Table 3**

CO<sub>2</sub> absorption rate at 10 min, apparent rate constant, CO<sub>2</sub> diffusivity, pKa value, and hydroxyl ion concentration of aq. DFILs. All calculation is done at 300 K and ambient pressure.

Absorbent	$-r_a \text{ (10 min)} * 10^{-2} \text{ (mol l}^{-1} \text{ min}^{-1}\text{)}$	$K_{app} * 10^{-2} \text{ (min}^{-1}\text{)}$	$D_{CO_2,fl} * 10^{-9} \text{ (m}^2/\text{s)}$	pKa	Before CO <sub>2</sub> loading [OH] <sup>-</sup> (mol/l) *	After CO <sub>2</sub> loading [OH] <sup>-</sup> (mol/l) *
Aq. [TETAH] [Pz]	3.95	2.33	1.786	10.19	9.55	4.90
Aq. [TETAH] [Tz]	2.67	2.12	1.775	7.32	3.55	3.31
Aq. [TETAH] [Py]	3.00	2.28	1.790	10.82	19.50	4.47
Aq. [TETAH] [Im]	3.35	2.29	1.792	10.90	21.38	5.13

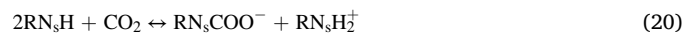
**Fig. 7.** pH value of CO<sub>2</sub> absorbents including DI water.

between CO<sub>2</sub> loading and CO<sub>2</sub> diffusivity is drawn and shown in **Fig. 8(a)**. The figure shows that CO<sub>2</sub> loading increases with increasing CO<sub>2</sub> diffusivity and CO<sub>2</sub> diffusivity of [TETAH][Pz] is marginally lower than [TETAH][Im] and [TETAH][Py]. A similar result is found when studying the relationship between CO<sub>2</sub> loading and pKa are shown in **Fig. 8(b)**. Alkalinity has a considerable influence on CO<sub>2</sub> loading in CO<sub>2</sub>-DFILs system as also reported by Y. Xu et al. work [31]. The alkalinity of an aqueous solution increases when carbonate and bicarbonate formation increases [54–56]. The pKa calculation shows that [OH]<sup>-</sup> ion formation in [TETAH][Im] and it reacts with CO<sub>2</sub> to form bicarbonate. Since alkalinity is high in [TETAH][Im], CO<sub>2</sub> loading is expected to be high in [TETAH][Im], but interestingly, CO<sub>2</sub> loading was found to be higher in [TETAH][Pz] which may be attributed to the high amount carbamate formation in CO<sub>2</sub>-[TETAH][Pz] system. A relationship was established between pKa values, and CO<sub>2</sub> diffusivities in DFILs and is plotted in **Fig. 8(c)**. The figure shows approximate linear relationship with value of R<sup>2</sup> is 0.9608. In the next section, a detailed study will be discussed about the formation of carbamates as well as bicarbonate in CO<sub>2</sub>-DFILs system based on <sup>13</sup>C NMR results.

### 3.5. Mechanism and interaction of CO<sub>2</sub>-DFILs system

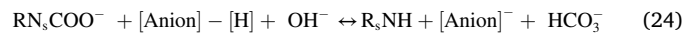
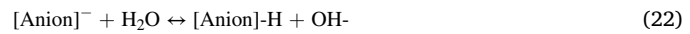
The mechanism of CO<sub>2</sub> absorption in the aq. DFILs, [TETAH][Im] and [TETAH][Pz] was studied using <sup>13</sup>C NMR spectroscopy. <sup>13</sup>C NMR results of aqueous and as-synthesized [TETAH][Im] with and without CO<sub>2</sub> reaction respectively are shown in **Fig. 9(a)** and for [TETAH][Pz], these results are shown in **Fig. 9(b)**. [TETAH] cation is bounded with four amines (three active amines group left) that can react with CO<sub>2</sub> to form carbamate. But the steric hindrance effect resists the formation of carbamates. In as-synthesized [TETAH][Im], a single peak of carbamate is found at the chemical shift ( $\delta$ ) 164.57 ppm, and this is a cation based carbamate, which means, no reaction between imidazole anion and CO<sub>2</sub> takes place. In the case of [TETAH][Pz], an extra peak at ( $\delta$ ) 163.03 ppm

of carbamate is obtained, which may be due to the reaction of piperazine anion with CO<sub>2</sub>. One extra peak is obtained in [TETAH][Pz], which confirmed that the effect of steric hindrance is lower in [TETAH][Pz]. Based on these results and literature [32,43,59], the reaction of cation (secondary amine) and anion (piperazine) with CO<sub>2</sub> may be expressed as follows:



In aqueous medium, <sup>13</sup>C results show that number of peaks (noise effect due to presence of water) increased, and this indicates decrease in steric hindrance in an aqueous medium. In aqueous [TETAH][Im], three carbamate peaks at ( $\delta$ ) 164.81, 164.55, and 164.12 ppm were obtained when amines in cation reacted with CO<sub>2</sub> and a new single peak obtained at ( $\delta$ ) 160.32 ppm indicates the formation of bicarbonate. Further, for aqueous [TETAH][Pz], one extra peak at ( $\delta$ ) 162.25 ppm is obtained as compared to aqueous [TETAH][Im], which confirms the formation of carbamate due to reaction between anion (piperazine) and CO<sub>2</sub>. The position of peaks in as-synthesized and aqueous DFILs are slightly different, which may be due to the presence of hydroxyl ions and carbonates. The intensity of bicarbonate peak in the range of ( $\delta$ ) 160.23–160.44 ppm is much higher than carbamates peaks in the range of ( $\delta$ ) 162–165 ppm. This shows that the formation of bicarbonates is high in CO<sub>2</sub>-DFILs system due to active sites. Based on these results, an expected CO<sub>2</sub> interaction in aqueous [TETAH][Pz] and [TETAH][Im] is shown in **Fig. 10** and **Fig. SI-7** respectively. CO<sub>2</sub> loading in [TETAH][Pz] is high due to the ease of formation of carbamates in it compared to other CO<sub>2</sub>-DFILs system.

Based on the NMR characterization and similar literature reports [36,60], the following reaction scheme consisting of hydrolysis of anion, formation of bicarbonate, and regeneration of DFILs, as given in Eqs. (22)–(24), respectively, is proposed.



DFILs regeneration as per Eq. (24) seems to be very evident in our system.

Further, to investigate the effect of CO<sub>2</sub> on anions, geometry optimization simulation technique was used to calculate the bond gap, and bond angle of CO<sub>2</sub>-anions system [61,62]. The value of bond gap between C–N is low in CO<sub>2</sub>-piperazine system (CO<sub>2</sub>-Pz) 1.462 Å compared to CO<sub>2</sub>-imidazole system (CO<sub>2</sub>-Im) 1.707 Å as mention in **Fig. 11(a)** and (b), respectively. The higher molecular attraction always causes to decrement in the bond gaps of molecules. Therefore, CO<sub>2</sub> attraction in CO<sub>2</sub>-piperazine system is higher than CO<sub>2</sub>-imidazole system. This attraction of CO<sub>2</sub> also reduces the bond angle of O–C–O from 180° to 139.552° and 130.132° for CO<sub>2</sub>-imidazole and piperazine system, respectively. These provide strong evidence that CO<sub>2</sub> loading in

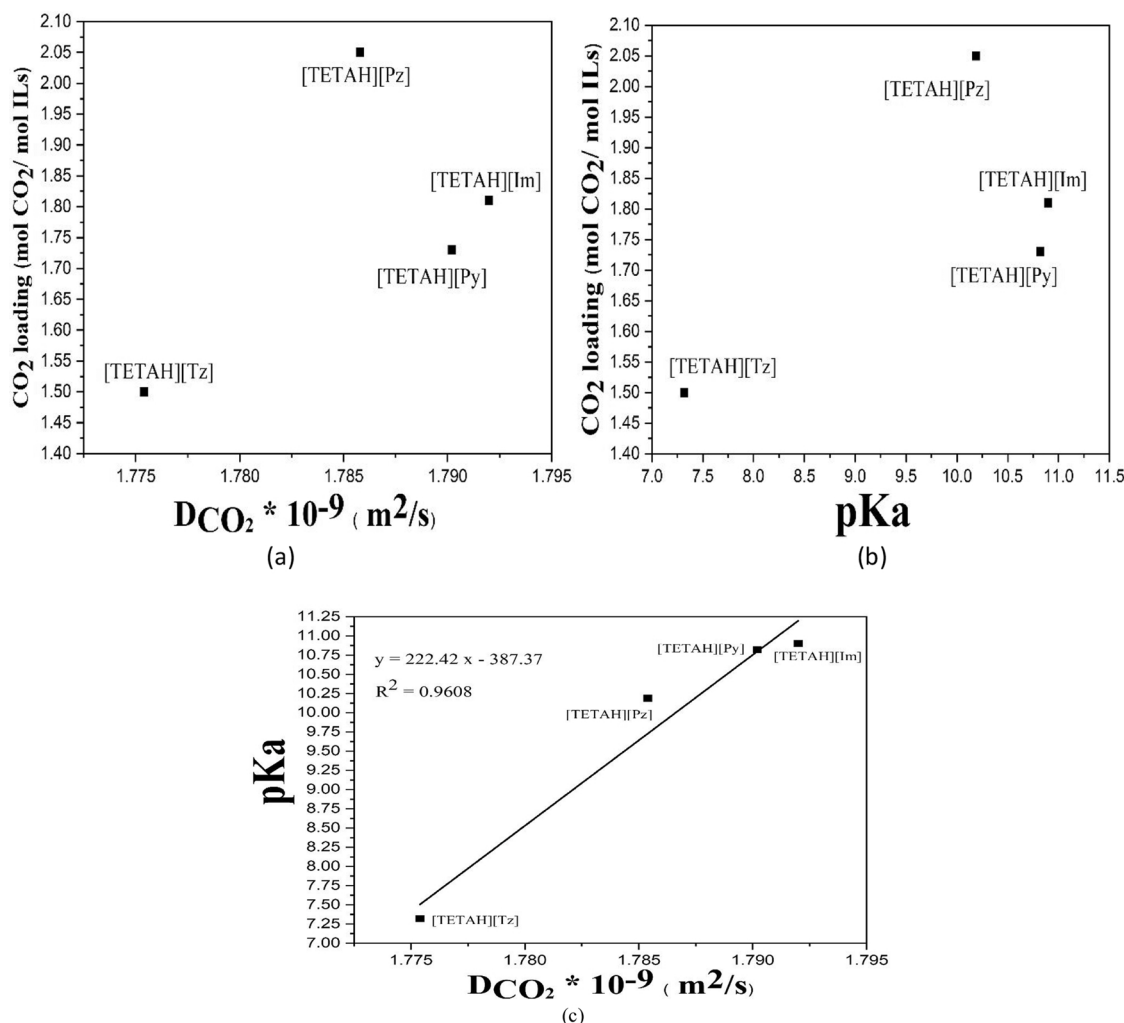


**Fig. 8.** Influence of CO<sub>2</sub> diffusivity into CO<sub>2</sub> loading (a), Influence of pKa value into CO<sub>2</sub> loading (b), and pKa and CO<sub>2</sub> diffusivity relationship (c) for the CO<sub>2</sub>-aqueous DFILs system.

[TETAH][Pz] is high compared to that in [TETAH][Im] and other DFILs. From Fig. 10, it is also seen that every amine group can react with CO<sub>2</sub> to form carbamates and bicarbonate in the presence of H<sub>2</sub>O. If the steric hindrance is reduced, and CO<sub>2</sub> pressure increased, the solubility will be increased from 2 to 3 mol CO<sub>2</sub> / mol DFIL.

### 3.6. Cyclic absorption capacity and regenerability of DFILs

The energy consumption in the regeneration of CO<sub>2</sub> from the absorbent is an important consideration for scale-up of the process to industrial scale [46,63]. Herein, regeneration of CO<sub>2</sub> rich aqueous DFILs was attempted at 393 K for 60 min time and is shown in Fig. 12. The initial rate of CO<sub>2</sub> desorption is high for all absorbents due to the rapid release of aqueous CO<sub>2</sub>. The steric hindrance effect causes formation of less stable compounds/ ions, which helps lowering the energy required for regeneration of CO<sub>2</sub> rich absorbent. From the figure, the CO<sub>2</sub> loading (mol of CO<sub>2</sub> / mol of IL) in the DFILs reduced to 0.264, 0.371, 0.429 and 0.563 in [TETAH][Tz], [TETAH][Py], [TETAH][Im] and [TETAH][Pz] respectively after desorption. Absorption capacity (mol of CO<sub>2</sub> / mol of ILs) of these aqueous DFILs was calculated as difference between CO<sub>2</sub> rich absorbent loading and CO<sub>2</sub> lean absorbent loading. The absorption capacity of [TETAH][Pz] is highest with 1.48 mol of CO<sub>2</sub> / mol of IL followed by 1.38, 1.36 and 1.24 mol of CO<sub>2</sub> / mol of IL for [TETAH][Im], [TETAH][Py], and [TETAH][Tz], respectively. Overall, the regeneration efficiency of all the DFILs absorbents is high.

The cyclic absorption capacity of these aqueous DFILs was also checked and is shown in Fig. 13. The cyclic capacity of all absorbents is found to be in the range of 96.51%–89.95 %, which indicates negligible loss of DFILs during four cycles (0.077 to 0.10 g/ gILs). The cyclic capacity of [TETAH][Tz] is marginally higher in the range of 96.51–92.26% for multiple absorption/desorption cycles, which may be due to the presence of hydrogen bonding. Further, the cyclic regeneration efficiency of absorbents (defined as the ratio of CO<sub>2</sub> loading after regeneration to that on fresh absorbent) was calculated, and found to be 94.43, 96.51, 94.09, and 93.84 for [TETAH][Pz], [TETAH][Tz], [TETAH][Py], and [TETAH][Im] respectively after the first cycle. The initial loss of absorbents is very small, around 4–7% is observed due to a few unstable compounds/ ions present in CO<sub>2</sub> rich absorbents that are removed along with CO<sub>2</sub> during regeneration. This loss of absorbent also was not noticed in the second and successive cycles, as the less stable compounds/ ions got removed initially. Overall, these lab synthesized DFILs have shown great potential to replace industrial amines based on their impressive absorption capacity.

### 4. Conclusion

In this work, a new class of dual functionalized ionic liquids were successfully synthesized in the laboratory and characterized successfully using <sup>1</sup>H and <sup>13</sup>C NMR, FTIR and TGA for their structure, functional groups and thermal stability respectively. Their viscosities over different

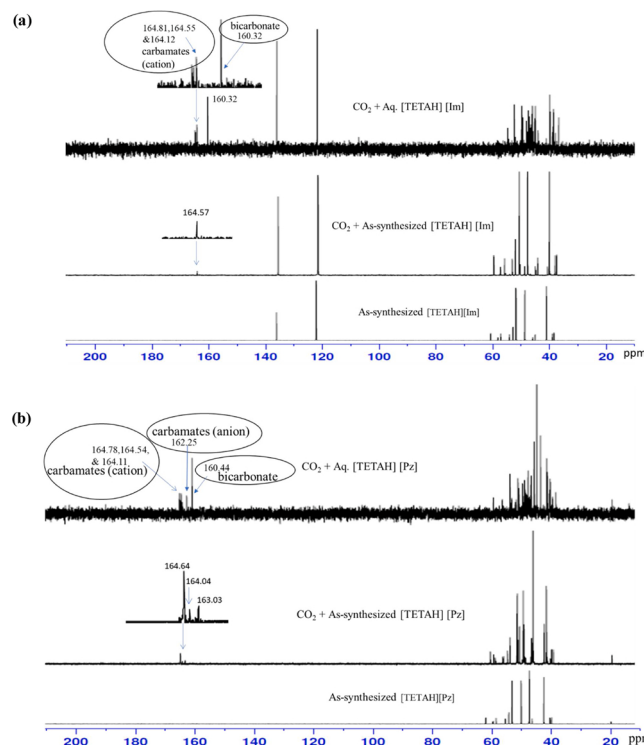


**Fig. 9.** (a). <sup>13</sup>C NMR spectra of CO<sub>2</sub> absorption in [TETAH][Im]. (b). <sup>13</sup>C NMR spectra of CO<sub>2</sub> absorption in [TETAH][Pz].

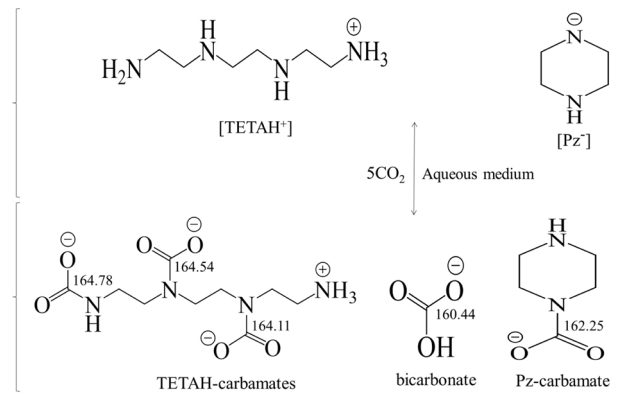


**Fig. 10.** Proposed CO<sub>2</sub> interaction with aqueous [TETAH][Pz] mechanism.

temperature ranges were measured and found to rapidly decrease with increasing temperature. CO<sub>2</sub> solubility is high in all the aqueous DFILs with highest loading of 2.05 mol of CO<sub>2</sub> / mol of IL for [TETAH][Pz].

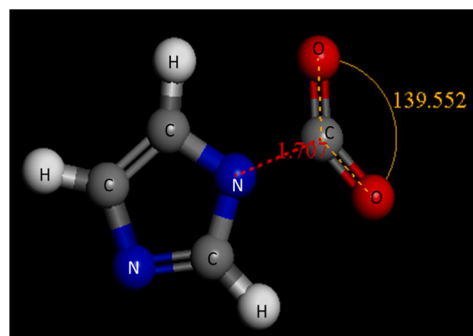


**Fig. 11.** (a) Geometry optimized CO<sub>2</sub>-Im system (b) Geometry optimized CO<sub>2</sub>-Pz system.

Based on molar concentration of hydroxyl ion, the formation of bicarbonates is higher in [TETAH][Im] and [TETAH][Py]. Further, it is seen that alkalinity plays a crucial role in enhancing CO<sub>2</sub> solubility in DFILs. <sup>13</sup>C NMR results reveals that the influence of steric hindrance in as-synthesized DFILs is strong, and this effect was reduced in an aqueous medium. <sup>13</sup>C NMR results also confirmed formation of carbamates in [TETAH][Pz] is higher, which reflects in its high CO<sub>2</sub> absorption capacity. Geometry optimization simulation technique was also used to calculate the bond gap, and bond angle of CO<sub>2</sub>-anions system and the results of the calculation could further explain the high performance of [TETAH][Pz] as a carbon dioxide absorbent. The cyclic absorption capacity of these aq. DFILs is also determined and found to be around

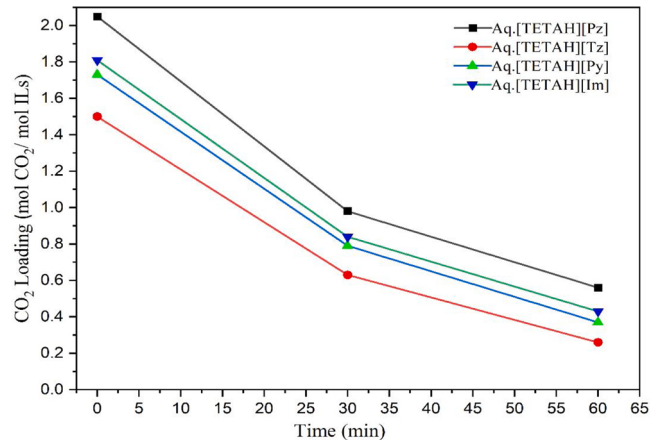


**Fig. 12.** CO<sub>2</sub> desorption in aqueous DFILs (at 393 K and ambient pressure).

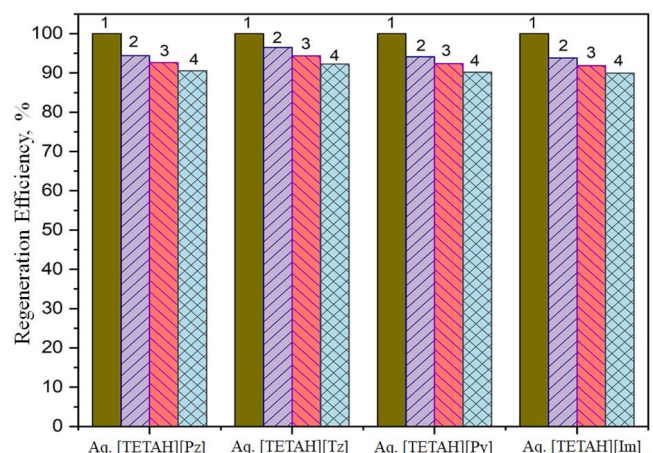
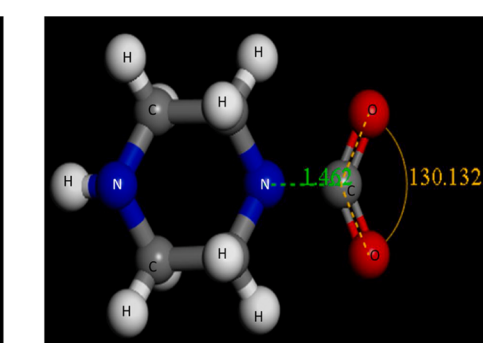


**Fig. 13.** CO<sub>2</sub> regeneration cycles of aqueous DFILs.



96–90 % with highest for [TETAH][Tz]. These DFILs were also found to be easily regenerated with negligible losses upto four regeneration cycles and hence, show promise as future carbon dioxide absorbents from industrial effluent flue gases.

## Declaration of Competing Interest

The authors declare that they have no known competing financial interests or personal relationships that could have appeared to influence the work reported in this paper.

## Acknowledgments

Results presented in this work are part of the comprehensive project from the Department of Science and Technology, Government of India, entitled “Methanol Production from Indian Coal: Pilot Plant Demonstration, Catalysis and Scale-up Technologies” (Sanction Order No.: TMD/CERI/MDME/2017/001). The author Sreedevi Upadhyayula also acknowledges the funding of Grant No. DST/TM/EWO/MI/CCUS/28 (G1) dtd. 28.09.2019 from the Department of Science and Technology, Ministry of Human Resource Development, New Delhi, India. The authors acknowledge Prof. Naresh Bhatnagar, Department of Mechanical Engineering, IIT Delhi, for their needful help.

## Appendix A. Supplementary data

Supplementary material related to this article can be found, in the online version, at doi:<https://doi.org/10.1016/j.jcou.2020.101416>.

## References

- [1] I.E. Agency, Global Energy and CO<sub>2</sub> Status Report INTERNATIONAL ENERGY, 2019.
- [2] J.B. Zhang, H. Peng, Y. Liu, D.J. Tao, P. Wu, J.P. Fan, K. Huang, Highly efficient CO<sub>2</sub> capture by polyethylenimine plus 1-ethyl-3-methylimidazolium acetate mixed absorbents, *ACS Sustain. Chem. Eng.* 7 (2019) 9369–9377.
- [3] J.O. Lloret, L.F. Vega, F. Llovel, A consistent and transferable thermodynamic model to accurately describe CO<sub>2</sub> capture with monoethanolamine, *J. CO<sub>2</sub> Util.* 21 (2017) 521–533.
- [4] B. Dutcher, M. Fan, A.G. Russell, Amine-based CO<sub>2</sub> capture technology development from the beginning of 2013- a review, *ACS Appl. Mater. Interfaces* 7 (4) (2015) 2137–2148.
- [5] S. Singto, T. Supap, R. Idem, P. Tontiwachwuthikul, S. Tantayanon, M.J. Al-Marri, A. Benamor, Synthesis of new amines for enhanced carbon dioxide (CO<sub>2</sub>) capture performance: the effect of chemical structure on equilibrium solubility, cyclic capacity, kinetics of absorption and regeneration, and heats of absorption and regeneration, *Sep. Purif. Technol.* 167 (2016) 97–107.
- [6] G. Cui, J. Wang, S. Zhang, Active chemisorption sites in functionalized ionic liquids for carbon capture, *Chem. Soc. Rev.* 45 (2016) 4307–4339.
- [7] K.R. Harris, M. Kanakubo, L.A. Woolf, Temperature and pressure dependence of the viscosity of the ionic liquid 1-butyl-3-methylimidazolium tetrafluoroborate: viscosity and density relationships in ionic liquids, *J. Chem. Eng. Data* 52 (6) (2007) 2425–2430.
- [8] M.D. Fayer, Dynamics and structure of room temperature ionic liquids, *Chem. Phys. Lett.* 616–617 (2014) 259–274.
- [9] M. Ramdin, T.W. De Loos, T.J.H. Vlugt, State-of-the-art of CO<sub>2</sub> capture with ionic liquids, *Ind. Eng. Chem. Res.* 51 (2012) 8149–8177.
- [10] B. Engineering, V. Uni, N. Dame, B.E. Gurkan, J.C. De Fuente, E.M. Mindrup, L. E. Ficke, B.F. Goodrich, E.A. Price, W.F. Schneider, J.F. Brennecke, Equimolar CO<sub>2</sub> absorption by anion-functionalized ionic liquids, *J. Am. Chem. Soc.* 132 (2010) 2116–2117.
- [11] Z.Z. Yang, Y.N. Zhao, L.N. He, CO<sub>2</sub>chemistry: Task-specific ionic liquids for CO<sub>2</sub> capture/activation and subsequent conversion, *RSC Adv.* 1 (2011) 545–567.
- [12] M. Aghaie, N. Rezaei, S. Zendehboudi, A systematic review on CO<sub>2</sub> capture with ionic liquids: current status and future prospects, *Renew. Sustain. Energy Rev.* 96 (2018) 502–525.
- [13] Y. Zhang, P. Yu, Y. Luo, Absorption of CO<sub>2</sub> by amino acid-functionalized and traditional dicationic ionic liquids: properties, Henry's law constants and mechanisms, *Chem. Eng. J.* 214 (2013) 355–363.
- [14] S. Shen, Y.N. Yang, Y. Bian, Y. Zhao, Kinetics of CO<sub>2</sub> absorption into aqueous basic amino acid salt: potassium salt of lysine solution, *Environ. Sci. Technol.* 50 (2016) 2054–2063.
- [15] Y. Zhang, S. Zhang, X. Lu, Q. Zhou, W. Fan, X.P. Zhang, Dual amino-functionalised phosphonium ionic liquids for CO<sub>2</sub> capture, *Chem. Eur. J.* 15 (2009) 3003–3011.
- [16] B. Lv, G. Jing, Y. Qian, Z. Zhou, An efficient absorbent of amine-based amino acid-functionalized ionic liquids for CO<sub>2</sub> capture: high capacity and regeneration ability, *Chem. Eng. J.* 289 (2016) 212–218.
- [17] Z. Zhou, X. Zhou, G. Jing, B. Lv, Evaluation of the multi-amine functionalized ionic liquid for efficient postcombustion CO<sub>2</sub> capture, *Energy Fuels* 30 (9) (2016) 7489–7495.
- [18] J. Albo, P. Luis, A. Irabien, Absorption of coal combustion flue gases in ionic liquids using different membrane contactors, *Desalin. Water Treat.* 27 (2011) 54–59.
- [19] J. Albo, P. Luis, A. Irabien, Carbon dioxide capture from flue gases using a cross-flow membrane contactor and the ionic liquid 1-ethyl-3-methylimidazolium ethylsulfate, *Ind. Eng. Chem. Res.* 49 (2010) 11045–11051.
- [20] Q. Sohaib, J.M. Vadillo, L. Gómez-Coma, J. Albo, S. Druon-Bocquet, A. Irabien, J. Sanchez-Marcano, CO<sub>2</sub> capture with room temperature ionic liquids; coupled absorption/desorption and single module absorption in membrane contactor, *Chem. Eng. Sci.* 223 (2020), 115719.
- [21] M. Pan, Y. Zhao, X. Zeng, J. Zou, Efficient absorption of CO<sub>2</sub> by introduction of intramolecular hydrogen bonding in chiral amino acid ionic liquids, *Energy Fuels* 32 (2018) 6130–6135.
- [22] T.B. Lee, S. Oh, T.R. Gohndrone, O. Morales-Collazo, S. Seo, J.F. Brennecke, W. F. Schneider, CO<sub>2</sub>chemistry of Phenolate-Based Ionic Liquids, *J. Phys. Chem. B* 120 (2016) 1509–1517.
- [23] K.E. Gutowski, E.J. Maginn, Amine-functionalized task-specific ionic liquids: a mechanistic explanation for the dramatic increase in viscosity upon complexation with CO<sub>2</sub> from molecular simulation, *J. Am. Chem. Soc.* 130 (2008) 14690–14704.
- [24] A. Li, Z. Tian, T. Yan, D.E. Jiang, S. Dai, Anion-functionalized task-specific ionic liquids: molecular origin of change in viscosity upon CO<sub>2</sub> capture, *J. Phys. Chem. B* 118 (2014) 14880–14887.
- [25] G. García, M. Atilhan, S. Aparicio, Water effect on acid-gas capture using choline lactate: a DFT insight beyond molecule-molecule pair simulations, *J. Phys. Chem. B* 119 (2015) 5546–5557.
- [26] S. Kang, Y.G. Chung, J.H. Kang, H. Song, CO<sub>2</sub> absorption characteristics of amino group functionalized imidazolium-based amino acid ionic liquids, *J. Mol. Liq.* 297 (2020), 111825.
- [27] X. Zhang, W. Xiong, Z. Tu, L. Peng, Y. Wu, X. Hu, Supported ionic liquid membranes with dual-site interaction mechanism for efficient separation of CO<sub>2</sub>, *ACS Sustain. Chem. Eng.* 7 (2019) 10792–10799.
- [28] E. Santos, J. Albo, A. Irabien, Acetate based supported ionic liquid membranes (SILMs) for CO<sub>2</sub> separation: influence of the temperature, *J. Memb. Sci.* 452 (2014) 277–283.
- [29] J. Albo, T. Yoshioka, T. Tsuru, Porous Al<sub>2</sub>O<sub>3</sub>/TiO<sub>2</sub> tubes in combination with 1-ethyl-3-methylimidazolium acetate ionic liquid for CO<sub>2</sub>/N<sub>2</sub> separation, *Sep. Purif. Technol.* 122 (2014) 440–448.
- [30] C. Wang, H. Luo, D.E. Jiang, H. Li, S. Dai, Carbon dioxide capture by superbase-derived protic ionic liquids, *Angew. Chemie Int. Ed.* 49 (2010) 5978–5981.
- [31] Y. Xu, CO<sub>2</sub> absorption behavior of azole-based protic ionic liquids: influence of the alkalinity and physicochemical properties, *J. CO<sub>2</sub> Util.* 19 (2017) 1–8.
- [32] C. Wang, X. Luo, H. Luo, D.E. Jiang, H. Li, S. Dai, Tuning the basicity of ionic liquids for equimolar CO<sub>2</sub> capture, *Angew. Chemie Int. Ed.* 50 (2011) 4918–4922.
- [33] X. Zhang, W. Xiong, L. Peng, Y. Wu, X. Hu, Highly selective absorption separation of H<sub>2</sub>S and CO<sub>2</sub> from CH<sub>4</sub> by novel azole-based protic ionic liquids, *AIChE J.* 66 (2020) 1–11.
- [34] T.J. Simons, T. Verheyen, E.I. Izgorodina, R. Vijayaraghavan, S. Young, A. K. Pearson, S.J. Pas, D.R. MacFarlane, Mechanisms of low temperature capture and regeneration of CO<sub>2</sub> using diamino protic ionic liquids, *Phys. Chem. Chem. Phys.* 18 (2016) 1140–1149.
- [35] T. Onsicik, R. Vijayaraghavan, D.R. Macfarlane, High CO<sub>2</sub> absorption by diamino protic ionic liquids using azolide anions, *Chem. Commun.* 54 (2018) 2106–2109.
- [36] J. Wu, B. Lv, X. Wu, Z. Zhou, G. Jing, Aprotic heterocyclic anion-based dual-functionalized ionic liquid solutions for efficient CO<sub>2</sub> uptake: quantum chemistry calculation and experimental research, *ACS Sustain. Chem. Eng.* 7 (2019) 7312–7323.
- [37] Y. Sun, S. Ren, Y. Hou, K. Zhang, W. Wu, Highly efficient absorption of NO by dual functional ionic liquids with low viscosity, *Ind. Eng. Chem. Res.* 58 (2019) 13313–13320.
- [38] P. Hu, R. Zhang, Z. Liu, H. Liu, C. Xu, X. Meng, M. Liang, S. Liang, Absorption Performance and Mechanism of CO<sub>2</sub>in Aqueous Solutions of Amine-Based Ionic Liquids, *Energy Fuels* 29 (2015) 6019–6024.
- [39] W. Conway, D. Fernandes, Y. Beyad, R. Burns, G. Lawrence, G. Puxty, M. Maeder, Reactions of CO<sub>2</sub> with aqueous piperazine solutions: formation and decomposition of mono- and dicarboxylic acids/carbamates of piperazine at 25.0 °C, *J. Phys. Chem. A* 117 (2013) 806–813.
- [40] X. Ma, I. Kim, R. Beck, H. Knuutila, J.P. Andreassen, Precipitation of piperazine in aqueous piperazine solutions with and without CO<sub>2</sub> loadings, *Ind. Eng. Chem. Res.* 51 (2012) 12126–12134.
- [41] Q. Liu, M. Yang, P.-P. Li, S.-S. Sun, U. Wlez-Biermann, Z.-C. Tan, Q.-G. Zhang, Physicochemical properties of ionic liquids [C<sub>3</sub>py][NTf<sub>2</sub>] and [C<sub>6</sub>py][NTf<sub>2</sub>], *J. Chem. Eng. Data* 56 (11) (2011) 4094–4101.
- [42] S.S. Moganty, R.E. Baltus, Regular solution theory for low pressure carbon dioxide solubility in room temperature ionic liquids: ionic liquid solubility parameter from activation energy of viscosity, *Ind. Eng. Chem. Res.* 49 (2010) 5846–5853.
- [43] X. Zhou, G. Jing, F. Liu, B. Lv, Z. Zhou, Mechanism and kinetics of CO<sub>2</sub> absorption into an aqueous solution of a triamino-functionalized ionic liquid, *Energy Fuels* 31 (2017) 1793–1802.
- [44] S. Liu, H. Ling, H. Gao, P. Tontiwachwuthikul, Z. Liang, H. Zhang, Kinetics and new Brønsted correlations study of CO<sub>2</sub> absorption into primary and secondary alkanolamine with and without steric-hindrance, *Sep. Purif. Technol.* 233 (2020), 115998.

- [45] S. Liu, H. Gao, C. He, Z. Liang, Experimental evaluation of highly efficient primary and secondary amines with lower energy by a novel method for post-combustion CO<sub>2</sub> capture, *Appl. Energy* 233–234 (2019) 443–452.
- [46] M. Xiao, H. Liu, H. Gao, W. Olson, Z. Liang, CO<sub>2</sub> capture with hybrid absorbents of low viscosity imidazolium-based ionic liquids and amine, *Appl. Energy* 235 (2019) 311–319.
- [47] C. Di Valentin, M. Freccero, R. Zanaletti, M. Sarzi-Amadè, o-Quinone methide as alkylating agent of nitrogen, oxygen, and sulfur nucleophiles. The role of H-bonding and solvent effects on the reactivity through a DFT computational study, *J. Am. Chem. Soc.* 123 (2001) 8366–8377.
- [48] S. Kumar, J.H. Cho, I. Moon, Ionic liquid-amine blends and CO<sub>2</sub> BOLs: prospective solvents for natural gas sweetening and CO<sub>2</sub> capture technology-A review, *Int. J. Greenh. Gas Control.* 20 (2014) 87–116.
- [49] E. Boli, T. Katsavrias, E. Voutsas, Viscosities of pure protic ionic liquids and their binary and ternary mixtures with water and ethanol, *Fluid Phase Equilib.* 520 (2020), 112663.
- [50] C.I. Daniel, J. Albo, E. Santos, C.A.M. Portugal, J.G. Crespo, A. Irabien, A group contribution method for the influence of the temperature in the viscosity of magnetic ionic liquids, *Fluid Phase Equilib.* 360 (2013) 29–35.
- [51] C. Li, A. Strachan, Cohesive energy density and solubility parameter evolution during the curing of thermoset, *Polymer (Guildf)* 135 (2018) 162–170.
- [52] P.W.J. Derkx, H.B.S. Dijkstra, J.A. Hogendoorn, G.F. Versteeg, Solubility of carbon dioxide in aqueous piperazine solution, *AIChE J.* 51 (2005) 2311–2327.
- [53] S.K. Dash, A. Samanta, A.N. Samanta, S.S. Bandyopadhyay, Vapour liquid equilibria of carbon dioxide in dilute and concentrated aqueous solutions of piperazine at low to high pressure, *Fluid Phase Equilib.* 300 (2011) 145–154.
- [54] B. Xie, Y. Xu, X. Tang, H. Shu, T. Chen, X. Zhu, Comparison of the alkalinity of hydroxypyridine anion-based protic ionic liquids and their catalytic performance for Knoevenagel reaction: the effect of the type of cation and the position of nitrogen atom of anion, *J. Mol. Liq.* 268 (2018) 610–616.
- [55] N.J.M.C. Penders-van Elk, S. Fradette, G.F. Versteeg, Effect of pKa on the kinetics of carbon dioxide absorption in aqueous alkanolamine solutions containing carbonic anhydrase at 298K, *Chem. Eng. J.* 259 (2015) 682–691.
- [56] K. Huang, Y.T. Wu, X.B. Hu, Effect of alkalinity on absorption capacity and selectivity of SO<sub>2</sub> and H<sub>2</sub>S over CO<sub>2</sub>: substituted benzoate-based ionic liquids as the study platform, *Chem. Eng. J.* 297 (2016) 265–276.
- [57] Octave Levenspiel, *Chemical Reaction Engineering*, 3rd ed., 1999, pp. 523–565. Ch. 23-24.
- [58] D. Eimer, *Gas Treating: Absorption Theory and Practice*, John Wiley & Sons, 2014.
- [59] G. Jing, Y. Qian, X. Zhou, B. Lv, Z. Zhou, Designing and screening of multi-amino-functionalized ionic liquid solution for CO<sub>2</sub> capture by quantum chemical simulation, *ACS Sustain. Chem. Eng.* 6 (2018) 1182–1191.
- [60] D. Xiong, G. Cui, J. Wang, H. Wang, Z. Li, K. Yao, S. Zhang, Reversible hydrophobic-hydrophilic transition of ionic liquids driven by carbon dioxide, *Angew. Chemie Int. Ed.* 54 (2015) 7265–7269.
- [61] J. Hu, L. Chen, M. Shi, C. Zhang, A quantum chemistry study for 1-ethyl-3-Methylimidazolium ion liquids with aprotic heterocyclic anions applied to carbon dioxide absorption, *Fluid Phase Equilib.* 459 (2018) 208–218.
- [62] X. Zhang, F. Huo, X. Liu, K. Dong, H. He, X. Yao, S. Zhang, Influence of microstructure and interaction on viscosity of ionic liquids, *Ind. Eng. Chem. Res.* 54 (2015) 3505–3514.
- [63] T.Q. Bui, S.G. Khokarale, S.K. Shukla, J.P. Mikkola, Switchable aqueous pentaethylenehexamine system for CO<sub>2</sub> capture: an alternative technology with industrial potential, *ACS Sustain. Chem. Eng.* 6 (2018) 10395–10407.